JCTC Journal of Chemical Theory and Computation

Article

pubs.acs.org/JCTC

Influence of Coupling and Embedding Schemes on QM Size Convergence in QM/MM Approaches for the Example of a Proton Transfer in DNA

Sven Roßbach[†,‡] and Christian Ochsenfeld*[,†,‡]

[†]Chair of Theoretical Chemistry, Department of Chemistry, University of Munich (LMU Munich), Butenandtstr. 7, D-81377 Munich, Germany

[‡]Center for Integrated Protein Science Munich (CIPSM) at the Department of Chemistry, University of Munich (LMU Munich), Butenandtstr, 5-13, D-81377 Munich, Germany

Supporting Information

ABSTRACT: The influence of embedding and coupling schemes on the convergence of the QM size in the QM/MM approach is investigated for the transfer of a proton in a DNA base pair. We find that the embedding scheme (mechanical or electrostatic) has a much greater impact on the convergence behavior than the coupling scheme (additive QM/MM or subtractive ONIOM). To achieve size convergence, QM regions with up to 6000 atoms are necessary for pure QM or mechanical embedding. In contrast, electrostatic embedding converges faster: for the example of the transfer of a proton between DNA base pairs, we recommend including at least five base pairs and 5 Å of solvent (including counterions) into the QM region, i.e., a total of 1150 atoms.

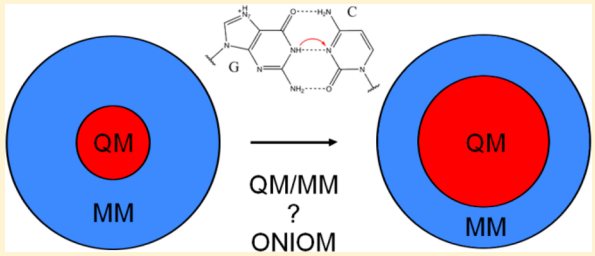

INTRODUCTION

Over the last 2 decades, the combined quantum mechanical/molecular mechanical (QM/MM) approach received increasing attention[1,2] as it became evident that small QM models in the gas phase are often insufficient to properly describe real systems. In particular, studies of large biomolecular systems and processes in explicit solvent often require models with thousands or even tens of thousands of atoms that cannot be treated quantum mechanically to date. The QM/MM approach usually leads to a better description of the system compared to a small pure QM model, as the environment is fully taken into account. Recently, it has been shown that large QM regions are also important within the QM/MM scheme and that energy differences converge much faster and are more stable with regard to the QM size when employing the QM/MM approach.[3−10]

There are two possible ways to describe the coupling between QM and MM: additive and subtractive (Figure 1). In the additive case, which we will abbreviate in the following as QM/MM, the energy is the sum of the MM energy (without all terms already described by QM), the QM energy, and the energy of an explicit coupling term.[1,11] In the subtractive case (ONIOM), the total energy consists of the MM energy of the full system, minus the MM energy of the QM region, plus the QM energy of the QM region.[12,13]

The (additive) QM/MM approach has the advantage that parameters for QM and link atoms, saturating covalent bonds between QM and MM, are unnecessary, as these are never described by the force field. The subtractive ONIOM approach requires accurate parameters for all atoms, including link atoms, because an MM calculation of the QM region is also necessary to avoid double counting. Without link atoms and with electrostatic embedding, dummy parameters could be used for the QM region. In the QM/MM approach, only one calculation is needed for each region, but the ONIOM approach allows for any number of layers, combining any methods, including only QM methods (QM/QM). While the QM/MM approach needs a special coupling term to treat the border, in the ONIOM approach, the coupling is described on the lower level with the aim that possible artifacts derived from link atoms are implicitly corrected if the force field can reproduce the QM energies for the link atoms.[14]

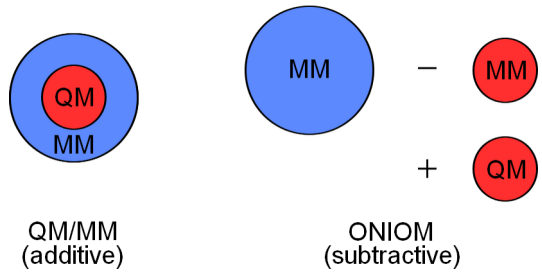

Figure 1. Schematic partitions by the additive QM/MM approach and the subtractive ONIOM method.

Received: July 21, 2016
Published: February 14, 2017

ACS Publications © 2017 American Chemical Society

DOI: 10.1021/acs.jctc.6b00727
J. Chem. Theory Comput. 2017, 13, 1102−1107

Independent of the coupling scheme, the QM region can be embedded in the MM region in different ways. Mechanical embedding treats the QM−MM interactions at the MM level, neglecting the mutual polarization of both regions. Electrostatic embedding includes the MM point charges into the QM calculation, allowing polarization of the QM region. Independent of the embedding scheme, QM size convergence within a QM/MM approach has been studied for different systems employing only the additive coupling scheme[3−7,10] or only the subtractive coupling scheme.[8,15−18]

We are interested in the influence of the

- coupling scheme: subtractive or additive
- embedding scheme: mechanical or electrostatic

on the QM size convergence. It has been suggested that the charges of the atoms in the QM region should be fitted based on the corresponding QM calculation.[17] However, in this work, the original mechanical embedding[12,19] has been employed. For our investigation, we chose an extensively studied proton transfer reaction within a DNA base pair (Figure 2), which has been repeatedly shown to require a larger QM region than previously expected:

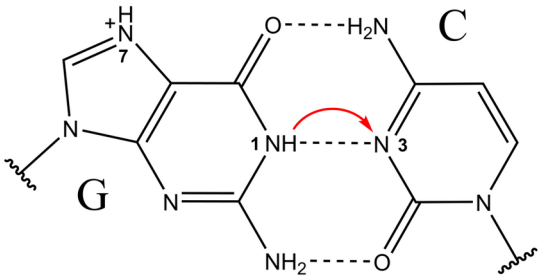

Figure 2. Single proton transfer within a protonated CG base pair, corresponding to residues 7 and 14 of the crystal structure.

In 1963, Löwdin[20] suggested "quantum jumps" (proton transfer) within base pairs as a source of mutations, which have been studied since then. Early calculations focused on the transfer of a single proton between the two bases in vacuum[21] or employed semiempirical methods to investigate double proton transfer.[22,23] Later, more accurate calculations employed perturbation theory or density-functional theory with increasing basis sets to study the stability of tautomers,[24−26] proton affinities of single bases,[25,27] and the dynamics of a base pair.[28−30] Nevertheless, single and double proton transfers between two base pairs have remained under investigation, with special attention given to the influence of a protonated base pair,[31,32] base stacking,[33−35] backbone and counterions,[33] and the solvent effect treated as a continuum model[24,25,28] or explicit microhydration.[26,33,36,37] It was suggested,[24] and later verified,[38] that the energetics of proton transfers also depend on the sequence. Therefore, very recent work added the adjacent base pairs to their models and included the solvent effect by explicit and/or implicit treatment of water.[39−41]

In our present work, we study systematically the QM size convergence of different embedding and coupling schemes for the example of the two DNA protonation states outlined above. Here, we investigate only the convergence behavior and not the absolute value of the energy difference itself.

COMPUTATIONAL DETAILS

Molecular Dynamics. The initial X-ray structure used for this work (1ZEW)[42] contains 10 base pairs of B-DNA. We used the LEAP module of AmberTools11[43] to add protons, neutralize the system with Na^+ ions, and solvate it in a box of TIP3P water with a buffer of 10 Å around the DNA, resulting in 13 127 atoms. Force field MD simulations were performed with the NAMD 2.10 package[44] and the AMBER10 force field. For the protonated nucleotides (Figure 2), GAFF parameters[45] were assigned with Antechamber.[46] Before the simulations, the solvent was optimized with 10 000 steps of conjugate gradient minimization, followed by another 10 000 steps, with restraints of 1 kcal/mol/Å^2 on the DNA. The system was heated to 300 K, increasing the temperature by 1 K/100 steps, while keeping the restraints. To allow a time step of 2 fs during equilibration, the SETTLE algorithm[47] was employed. Moreover, we used periodic boundary conditions, the particle mesh Ewald method,[48] Langevin dynamics for temperature control, and the Langevin piston Nosé−Hoover method for pressure control[49,50] (1 atm). The system was equilibrated for 400 ps, with restraints on the DNA, to obtain proper solvation. Residue 7 was then additionally protonated at N7, and the system was minimized again. To prepare the system after proton transfer, residue 7 was deprotonated at N1 and residue 14 was protonated at N3, followed by minimization of the bases.

QM Size Convergence. To study the convergence of the QM size, we calculated the energy difference of the two protonation states on the FF-minimized structures and systematically increased the QM region. We added base pairs until all 10 base pairs were included; then, we included water and ions based on the minimal distance of any atom to the DNA. Note that the absolute energy difference is not meaningful, as the structures are not reoptimized for any QM size. It has been shown that reoptimization of the geometries is not necessary to find the converged QM size[8,10] because single-point calculations follow the same trend and allow the calculation of larger QM regions. Moreover, as we model both protonation states, independent geometry optimizations would result in different conformations of the solvent and therefore lead to energy differences, which are mainly unrelated to proton transfer. Distance-based QM size convergence would thus become impossible. All QM calculations were performed with FermiONs++.[51,52]

ONIOM in ChemShell. In ChemShell,[11,53,54] the favored method to couple the QM and MM regions is by electrostatic embedding with the link atom approach in case there is a bond across the QM−MM border.[55] To avoid overpolarization of the link atom by the point charge of the neighboring MM atom, its charge is shifted to the next layer of MM atoms and the dipole moment is preserved by the addition of dipoles on these atoms.[11] To the "subtractive" module of ChemShell, we added the possibility of including electrostatic embedding with link atoms, shifted charges and dipoles in the MM calculation of the QM region. In this case, the dipoles are of the AMBER type EP and all residues containing link atoms need additional parameters, which are assigned by Antechamber[46] with RESP charges[56,57] at the B3LYP[58] level of theory with the 6-31G* basis set,[59,60] without structure reoptimization. The RESP charges were fitted on a grid of $N_{atoms} \times 2000$ points on the van der Waals shell scaled by 1.5.

DOI: 10.1021/acs.jctc.6b00727
J. Chem. Theory Comput. 2017, 13, 1102−1107

RESULTS AND DISCUSSION

Figure 3 shows the energy difference between the two protonation states with an increasing number of base pairs in the QM region for all combinations of the coupling and embedding schemes. While our focus here is on the convergence behavior and not on the value of ΔE (see Computational Details, QM Size Convergence), the most apparent differences in Figure 3 are the slow convergence of the ME scheme and that it seems to converge to a different ΔE than EE. In contrast, we find that the coupling scheme has only a minor influence on QM size convergence and that the first layer of adjacent base pairs has a very significant impact on ΔE, whereas in the case of EE, the influence of all base pairs beyond the second layer can be sufficiently described by point charges.

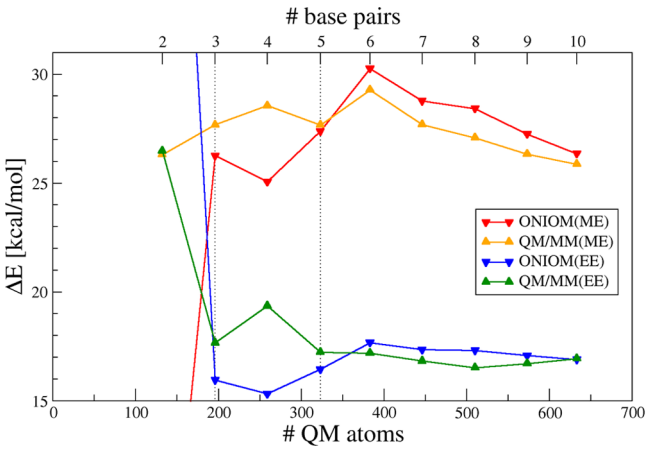

Figure 3. QM size convergence of additive (QM/MM) vs subtractive (ONIOM) coupling with mechanical (ME) and electrostatic (EE) embedding (M06-2X-D3/def2-SVP). The dashed lines show the first and second layers of base pairs around the proton transfer.

Further increasing the QM region to include solvent (water and Na^+ ions) eliminates the difference between the coupling schemes and shows that ME converges to the same ΔE as EE, but for ME, even 4000 QM atoms are not enough to reach size convergence (Figure 4).

Furthermore, no embedding scheme (pure QM) should also converge to the same energy difference as the QM−MM methods. Recent findings[3,7,8,61] showed that large energy fluctuations are usually expected when increasing the QM size in the gas phase before size convergence is reached. Typically, 1000 QM atoms are clearly sufficient, even though, depending on the accuracy, sometimes more than 1000 QM

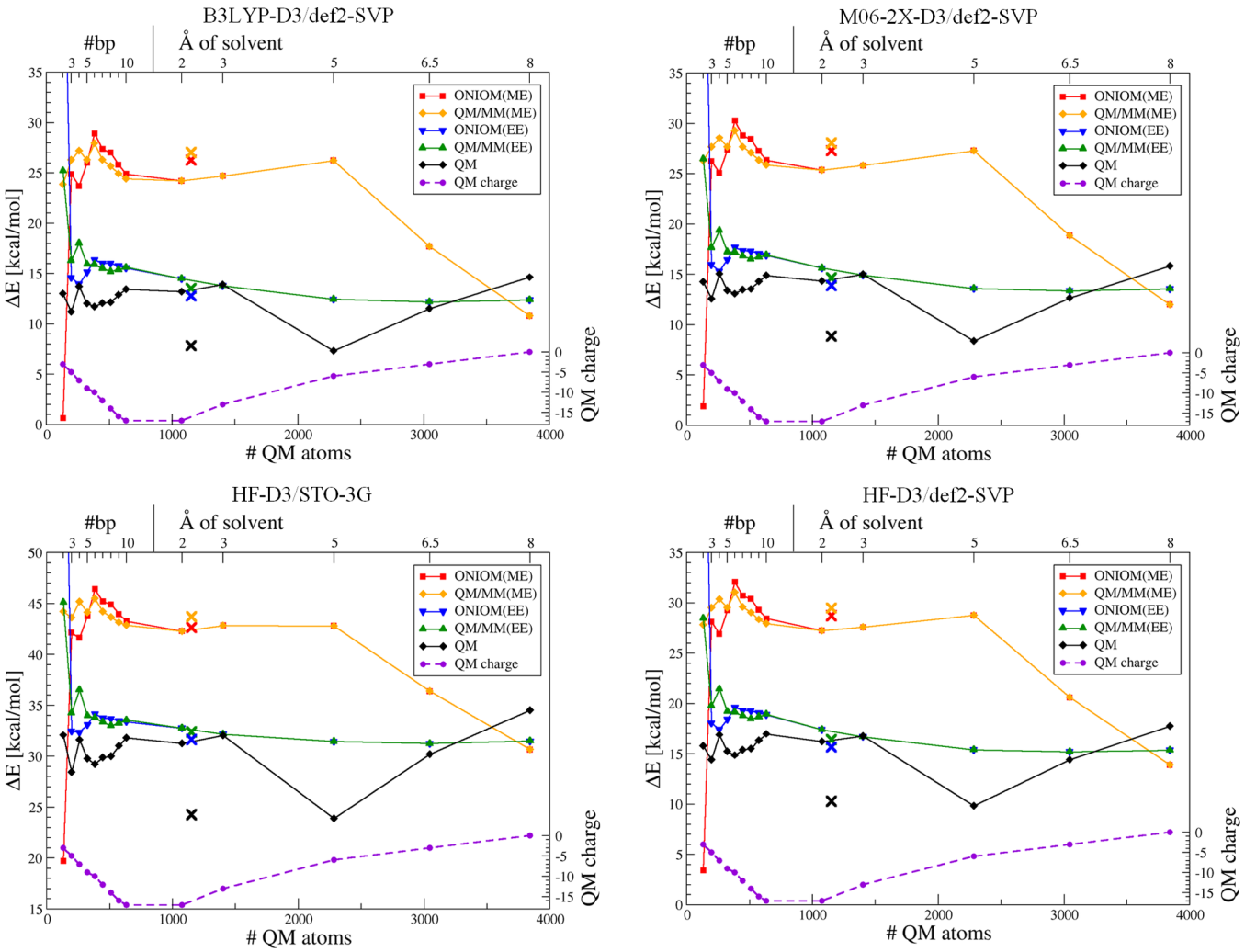

Figure 4. Comparison of QM size convergence for different method/basis set combinations. In addition, crosses show data for the QM region with five base pairs and 5 Å of solvent (water and ions).

DOI: 10.1021/acs.jctc.6b00727
J. Chem. Theory Comput. 2017, 13, 1102−1107

atoms are needed. In our case, ΔE(pure QM) seems to converge rather fast and becomes stable with fluctuations of less than 2.6 kcal/mol within 1000 atoms with def2-SVP[62] (Figure 4). However, further increasing the QM region shows that the apparent convergence is misleading and that oscillations occur beyond 1000 atoms; even 4000 atoms are not enough to converge ΔE(pure QM) with respect to the QM size. It seems that the total QM charge can have a significant influence on ΔE, although changes in the total QM charge do not necessarily lead to a change in the energy difference.

We find that the convergence behavior of different methods is quite independent of the choice of method and basis set when comparing B3LYP-D3,[58,63] M06-2X-D3,[63,64] and HF-D3 with an SVP basis. Even HF-D3/STO-3G shows basically the same picture, which allows us to further extend the QM region. The energy difference for pure QM finally converges to the same value as that with EE when we include 6000 atoms in the QM region (Figure 5). Additionally, ME finally converges to

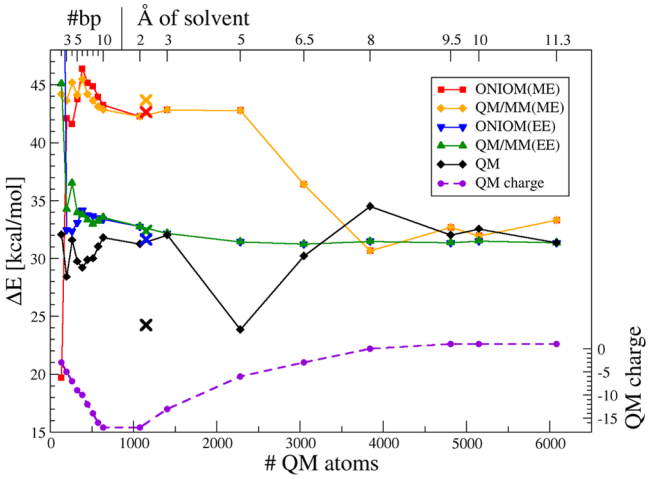

Figure 5. QM size convergence with up to 6000 QM atoms (HF-D3/STO-3G).

the same ΔE as that of EE and pure QM, but even with 6000 QM atoms, corresponding to 10 base pairs including 11.3 Å of solvent, ΔE(ME) differs by 2 kcal/mol from ΔE(EE) (Figure 5).

On the basis of these (single point) QM size convergence calculations, we suggest that at least five base pairs of the DNA double strand with 5 Å of solvent around these base pairs are necessary within the QM region to reach size convergence within 1 kcal/mol for the present system using electrostatic embedding. This leads to a QM region of about 1000 atoms (Figure 6). Although the exact size of the converged QM region presumably depends on the positions of the counterions, these results are in good agreement with the "big-QM approach" for proteins by Sumner et al.,[8] who suggested the inclusion of all atoms within 4.5 Å of the minimal active site and the movement of junctions at least three residues away. For our DNA system, we find that it is not necessary to include charged groups/ions of the solvent into the QM region in the case of EE. ME and pure QM calculations would benefit from the inclusion of all ions into the QM region; however, such a scheme would not be in line with the typically preferred approach of increasing the QM sphere progressively based on the distance (see also SI-2). The ME scheme can be improved by atomic charges derived from the QM calculation, which

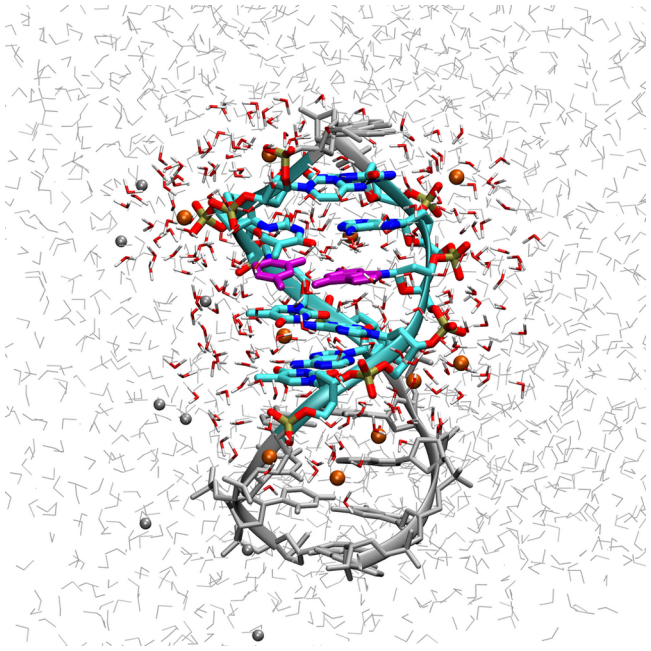

Figure 6. Cutout of the system. The suggested QM region, consisting of five base pairs surrounded by 5 Å of solvent, is shown in color. The protonated base pair (Figure 2) is highlighted in magenta. Atoms treated at the MM level are shown in gray. Protons of the DNA are not shown for clarity. Counterions are represented by balls.

recover polarization effects within the QM region.[17,65] Although the QM size convergence behavior can also be improved by this approach, no general scheme to derive QM enhanced charges has been suggested so far that is applicable to QM size convergence (see SI-3). Moreover, none of the tested variations of ME converged faster with the QM size than EE.

CONCLUSIONS

We showed that the choice of the coupling scheme between the QM and MM parts has no significant influence on the size of the converged QM region; however, the embedding scheme is important. Mechanical embedding, as in the original ONIOM approach, can result in slow convergence with misleading energies, even for large QM sizes, whereas electrostatic embedding leads to fast and reliable convergence of the QM size. No embedding (pure QM) can lead to seemingly fast size convergence that can only be identified as erroneous with very large QM regions. We find that, for the present system, the converged QM size is nearly independent of the chosen method/basis. Therefore, we conclude that QM sizes with no fewer than two adjacent base pairs on each side and at least 5 Å of solvent around these base pairs should ideally be employed for a reliable description of proton transfer processes within a DNA base pair, i.e., a total of 1150 QM atoms.

ASSOCIATED CONTENT

Supporting Information

The Supporting Information is available free of charge on the ACS Publications website at DOI: 10.1021/acs.jctc.6b00727.

Data from Figures 3−5 in tabular form, additional information on the influence of counterions on the QM size convergence of ME and pure QM, additional information on the QM size convergence with QM enhanced charges (PDF)

DOI: 10.1021/acs.jctc.6b00727
J. Chem. Theory Comput. 2017, 13, 1102−1107

Coordinates of the systems before proton transfer (PDB)
Coordinates of the systems after proton transfer (PDB)

AUTHOR INFORMATION

Corresponding Author

*E-mail: christian.ochsenfeld@uni-muenchen.de.

ORCID

Christian Ochsenfeld: 0000-0002-4189-6558

Funding

We acknowledge financial support by the Volkswagen Stiftung within the funding initiative "New Conceptual Approaches to Modeling and Simulation of Complex Systems", and the DFG cluster of excellence EXC 114 "Center for Integrative Protein Science Munich" (CIPSM), and SFB 749.

Notes

The authors declare no competing financial interest.

REFERENCES

(1) Senn, H. M.; Thiel, W. QM/MM Methods for Biomolecular Systems. *Angew. Chem., Int. Ed.* **2009**, *48*, 1198−1229.
(2) Warshel, A. Multiscale Modeling of Biological Functions: From Enzymes to Molecular Machines (Nobel Lecture). *Angew. Chem., Int. Ed.* **2014**, *53*, 10020−10031.
(3) Sumowski, C. V.; Ochsenfeld, C. A Convergence Study of QM/MM Isomerization Energies with the Selected Size of the QM Region for Peptidic Systems. *J. Phys. Chem. A* **2009**, *113*, 11734−11741.
(4) Sumowski, C. V.; Schmitt, B. B. T.; Schweizer, S.; Ochsenfeld, C. Quantum-Chemical and Combined Quantum-Chemical/Molecular-Mechanical Studies on the Stabilization of a Twin Arginine Pair in Adenovirus Ad11. *Angew. Chem., Int. Ed.* **2010**, *49*, 9951−9955.
(5) van der Kamp, M. W.; Zurek, J.; Manby, F. R.; Harvey, J. N.; Mulholland, A. J. Testing High-Level QM/MM Methods for Modeling Enzyme Reactions: Acetyl-CoA Deprotonation in Citrate Synthase. *J. Phys. Chem. B* **2010**, *114*, 11303−11314.
(6) Liao, R. Z.; Thiel, W. Comparison of QM-Only and QM/MM Models for the Mechanism of Tungsten-Dependent Acetylene Hydratase. *J. Chem. Theory Comput.* **2012**, *8*, 3793−3803.
(7) Flaig, D.; Beer, M.; Ochsenfeld, C. Convergence of Electronic Structure with the Size of the QM Region: Example of QM/MM NMR Shieldings. *J. Chem. Theory Comput.* **2012**, *8*, 2260−2271.
(8) Sumner, S.; Söderhjelm, P.; Ryde, U. Effect of Geometry Optimizations on QM-Cluster and QM/MM Studies of Reaction Energies in Proteins. *J. Chem. Theory Comput.* **2013**, *9*, 4205−4214.
(9) Liao, R.-Z.; Thiel, W. Convergence in the QM-Only and QM/MM Modeling of Enzymatic Reactions: A Case Study for Acetylene Hydratase. *J. Comput. Chem.* **2013**, *34*, 2389−2397.
(10) Blank, I. D.; Sadeghian, K.; Ochsenfeld, C. A Base-Independent Repair Mechanism for DNA Glycosylase—No Discrimination Within the Active Site. *Sci. Rep.* **2015**, *5*, 10369.
(11) Sherwood, P.; de Vries, A. H.; Guest, M. F.; Schreckenbach, G.; Catlow, C. R. A.; French, S. A.; Sokol, A. A.; Bromley, S. T.; Thiel, W.; Turner, A. J.; Billeter, S.; Terstegen, F.; Thiel, S.; Kendrick, J.; Rogers, S. C.; Casci, J.; Watson, M.; King, F.; Karlsen, E.; Sjøvoll, M.; Fahmi, A.; Schäfer, A.; Lennartz, C. QUASI: A General Purpose Implementation of the QM/MM Approach and Its Application to Problems in Catalysis. *J. Mol. Struct.: THEOCHEM* **2003**, *632*, 1−28.
(12) Svensson, M.; Humbel, S.; Froese, R. D. J.; Matsubara, T.; Sieber, S.; Morokuma, K. ONIOM: A Multilayered Integrated MO + MM Method for Geometry Optimizations and Single Point Energy Predictions. A Test for Diels-Alder Reactions and Pt(P(t-Bu)3)2 + H2 Oxidative Addition. *J. Phys. Chem.* **1996**, *100*, 19357−19363.
(13) Chung, L. W.; Sameera, W. M. C.; Ramozzi, R.; Page, A. J.; Hatanaka, M.; Petrova, G. P.; Harris, T. V.; Li, X.; Ke, Z.; Liu, F.; Li, H.; Ding, L.; Morokuma, K. The ONIOM Method and Its Applications. *Chem. Rev.* **2015**, *115*, 5678−5796.
(14) Vreven, T.; Byun, K. S.; Komáromi, I.; Dapprich, S.; Montgomery, J. A., Jr.; Morokuma, K.; Frisch, M. J. Combining Quantum Mechanics Methods with Molecular Mechanics Methods in ONIOM. *J. Chem. Theory Comput.* **2006**, *2*, 815−826.
(15) Kaukonen, M.; Söderhjelm, P.; Heimdal, J.; Ryde, U. Proton Transfer at Metal Sites in Proteins Studied by Quantum Mechanical Free-Energy Perturbations. *J. Chem. Theory Comput.* **2008**, *4*, 985−1001.
(16) Hu, L.; Eliasson, J.; Heimdal, J.; Ryde, U. Do Quantum Mechanical Energies Calculated for Small Models of Protein-Active Sites Converge? *J. Phys. Chem. A* **2009**, *113*, 11793−11800.
(17) Hu, L.; Söderhjelm, P.; Ryde, U. On the Convergence of QM/MM Energies. *J. Chem. Theory Comput.* **2011**, *7*, 761−777.
(18) Du, L.; Gao, J.; Liu, Y.; Zhang, D.; Liu, C. The Reaction Mechanism of Hydroxyethylphosphonate Dioxygenase: A QM/MM Study. *Org. Biomol. Chem.* **2012**, *10*, 1014−1024.
(19) Bakowies, D.; Thiel, W. Hybrid Models for Combined Quantum Mechanical and Molecular Mechanical Approaches. *J. Phys. Chem.* **1996**, *100*, 10580−10594.
(20) Löwdin, P.-O. Proton Tunneling in DNA and Its Biological Implications. *Rev. Mod. Phys.* **1963**, *35*, 724−732.
(21) Clementi, E.; Mehl, J.; von Niessen, W. Study of the Electronic Structure of Molecules. XII. Hydrogen Bridges in the Guanine−Cytosine Pair and in the Dimeric Form of Formic Acid. *J. Chem. Phys.* **1971**, *54*, 508.
(22) Scheiner, S.; Kern, C. W. Theoretical Study of Proton Transfers Between Base Pairs of DNA. *Chem. Phys. Lett.* **1978**, *57*, 331−333.
(23) Lipinski, J.; Gorzkowska, E. Double Proton Transfer and Charge-Transfer Transitions in Biological Hydrogen-Bonded Systems. Guanine-Cytosine (G-C) and G-C-Mg2+ Systems. *Chem. Phys. Lett.* **1983**, *94*, 479−482.
(24) Florian, J.; Leszczynski, J. Spontaneous DNA Mutations Induced by Proton Transfer in the Guanine-Cytosine Base Pairs: An Energetic Perspective. *J. Am. Chem. Soc.* **1996**, *118*, 3010−3017.
(25) Colominas, C.; Luque, F. J.; Orozco, M. Tautomerism and Protonation of Guanine and Cytosine. Implications in the Formation of Hydrogen-Bonded Complexes. *J. Am. Chem. Soc.* **1996**, *118*, 6811−6821.
(26) Zhanpeisov, N. U.; Leszczynski, J. Specific Solvation Effects on the Structures and Properties of Neutral and One-Electron Oxidized Formamidine-Formamide Complexes. A Theoretical Ab Initio Study. *J. Phys. Chem. A* **1999**, *103*, 8317−8327.
(27) Chandra, A. K.; Nguyen, M. T.; Uchimaru, T.; Zeegers-Huyskens, T. Protonation and Deprotonation Enthalpies of Guanine and Adenine and Implications for the Structure and Energy of Their Complexes with Water: Comparison with Uracil, and Cytosine. *J. Phys. Chem. A* **1999**, *103*, 8853−8860.
(28) Zoete, V.; Meuwly, M. Double Proton Transfer in the Isolated and DNA-Embedded Guanine-Cytosine Base Pair. *J. Chem. Phys.* **2004**, *121*, 4377−4388.
(29) Villani, G. Theoretical Investigation of Hydrogen Transfer Mechanism in the Guanine-Cytosine Base Pair. *Chem. Phys.* **2006**, *324*, 438−446.
(30) Xiao, S.; Wang, L.; Liu, Y.; Lin, X.; Liang, H. Theoretical Investigation of the Proton Transfer Mechanism in Guanine-Cytosine and Adenine-Thymine Base Pairs. *J. Chem. Phys.* **2012**, *137*, 195101.
(31) Noguera, M.; Sodupe, M.; Bertrán, J. Effects of Protonation on Proton-Transfer Processes in Guanine-Cytosine Watson-Crick Base Pairs. *Theor. Chem. Acc.* **2004**, *112*, 318−326.
(32) Noguera, M.; Sodupe, M.; Bertrán, J. Effects of Protonation on Proton Transfer Processes in Watson-Crick Adenine-Thymine Base Pair. *Theor. Chem. Acc.* **2007**, *118*, 113−121.
(33) Chen, H. Y.; Kao, C. L.; Hsu, S. C. N. Proton Transfer in Guanine- Cytosine Radical Anion Embedded in B-Form DNA. *J. Am. Chem. Soc.* **2009**, *131*, 15930−15938.
(34) Matsui, T.; Sato, T.; Shigeta, Y.; Hirao, K. Sequence-Dependent Proton-Transfer Reaction in Stacked GC Pair II: The Origin of Stabilities of Proton-Transfer Products. *Chem. Phys. Lett.* **2009**, *478*, 238−242.

DOI: 10.1021/acs.jctc.6b00727
J. Chem. Theory Comput. 2017, 13, 1102−1107

(35) Villani, G. Theoretical Investigation of the Coupling between Hydrogen Atoms Transfer and Stacking Interaction in Guanine-Cytosine Dimers. *Phys. Chem. Chem. Phys.* **2013**, *15*, 19242−19252.
(36) Cerón-Carrasco, J. P.; Requena, A.; Zúñiga, J.; Michaux, C.; Perpète, E. A.; Jacquemin, D. Intermolecular Proton Transfer in Microhydrated Guanine-Cytosine Base Pairs: A New Mechanism for Spontaneous Mutation in DNA. *J. Phys. Chem. A* **2009**, *113*, 10549−10556.
(37) Cerón-Carrasco, J. P.; Zúñiga, J.; Requena, A.; Perpète, E. A.; Michaux, C.; Jacquemin, D. Combined Effect of Stacking and Solvation on the Spontaneous Mutation in DNA. *Phys. Chem. Chem. Phys.* **2011**, *13*, 14584−14589.
(38) Matsui, T.; Sato, T.; Shigeta, Y. Sqeuence Dependent Proton-Transfer Reaction in Stacked GC Pair I: The Possibility of Proton-Transfer Reactions. *Int. J. Quantum Chem.* **2009**, *109*, 2168−2177.
(39) Lin, Y.; Wang, H.; Wu, Y.; Gao, S.; Schaefer, H. F., III Proton-Transfer in Hydrogenated Guanine-Cytosine Trimer Neutral Species, Cations, and Anions Embedded in B-Form DNA. *Phys. Chem. Chem. Phys.* **2014**, *16*, 6717−6725.
(40) Jacquemin, D.; Zúñiga, J.; Requena, A.; Céron-Carrasco, J. P. Assessing the Importance of Proton Transfer Reactions in DNA. *Acc. Chem. Res.* **2014**, *47*, 2467−2474.
(41) Cerón-Carrasco, J. P.; Jacquemin, D. DNA Spontaneous Mutation and Its Role in the Evolution of GC-Content: Assessing the Impact of the Genetic Sequence. *Phys. Chem. Chem. Phys.* **2015**, *17*, 7754−7760.
(42) Hays, F. A.; Teegarden, A.; Jones, Z. J. R.; Harms, M.; Raup, D.; Watson, J.; Cavaliere, E.; Ho, P. S. Correction for Hays et Al., How Sequence Defines Structure: A Crystallographic Map of DNA Structure and Conformation. *Proc. Natl. Acad. Sci. U. S. A.* **2010**, *107*, 4486−4486.
(43) Case, D. A.; Darden, T.; Cheatham, T. E., III; Simmerling, C.; Wang, J.; Duke, R. E.; Luo, R.; Walker, R. C.; Zhang, W.; Merz, K. M.; Roberts, B. P.; Hayik, S.; Roitberg, A.; Seabra, G.; Kolossváry, I.; Wong, K. F.; Paesani, F.; Vanicek, J.; Liu, J.; Wu, X.; Brozell, S. R.; Steinbrecher, T.; Gohlke, H.; Cai, Q.; Ye, X.; Wang, J.; Hsieh, M.-J.; Hornak, V.; Cui, G.; Roe, D. R.; Mathews, D. H.; Seetin, M. G.; Sagui, C.; Babin, V.; Luchko, T.; Gusarov, S.; Kovalenko, A.; Kollman, P. A. *Amber 11*; University of California: San Francisco, 2010.
(44) Phillips, J. C.; Braun, R.; Wang, W.; Gumbart, J.; Tajkhorshid, E.; Villa, E.; Chipot, C.; Skeel, R. D.; Kalé, L.; Schulten, K. Scalable Molecular Dynamics with NAMD. *J. Comput. Chem.* **2005**, *26*, 1781−1802.
(45) Wang, J.; Wolf, R.; Caldwell, J. W.; Kollman, P. A.; Case, D. A. Development and Testing of a General Amber Force Field. *J. Comput. Chem.* **2004**, *25*, 1157−1174.
(46) Wang, J.; Wang, W.; Kollman, P. A.; Case, D. A. Automatic Atom Type and Bond Type Perception in Molecular Mechanical Calculations. *J. Mol. Graphics Modell.* **2006**, *25*, 247−260.
(47) Miyamoto, S.; Kollman, P. A. SETTLE: An Analytical Version of the SHAKE and RATTLE Algorithm for Rigid Water Models. *J. Comput. Chem.* **1992**, *13*, 952−962.
(48) Darden, T.; Perera, L.; Li, L.; Pedersen, L. New Tricks for Modelers from the Crystallography Toolkit: The Particle Mesh Ewald Algorithm and Its Use in Nucleic Acid Simulations. *Structure* **1999**, *7*, 55−60.
(49) Martyna, G. J.; Tobias, D. J.; Klein, M. L. Constant Pressure Molecular Dynamics Algorithms. *J. Chem. Phys.* **1994**, *101*, 4177−4189.
(50) Feller, S. E.; Zhang, Y.; Pastor, R. W.; Brooks, B. R. Constant Pressure Molecular Dynamics Simulation: The Langevin Piston Method. *J. Chem. Phys.* **1995**, *103*, 4613−4621.
(51) Kussmann, J.; Ochsenfeld, C. Pre-Selective Screening for Matrix Elements in Linear-Scaling Exact Exchange Calculations. *J. Chem. Phys.* **2013**, *138*, 134114.
(52) Kussmann, J.; Ochsenfeld, C. Preselective Screening for Linear-Scaling Exact Exchange-Gradient Calculations for Graphics Processing Units and General Strong-Scaling Massively Parallel Calculations. *J. Chem. Theory Comput.* **2015**, *11*, 918−922.
(53) *ChemShell*, a Computational Chemistry Shell. www.chemshell.org.
(54) Kästner, J.; Carr, J. M.; Keal, T. W.; Thiel, W.; Wander, A.; Sherwood, P. DL-FIND: An Open-Source Geometry Optimizer for Atomistic Simulations. *J. Phys. Chem. A* **2009**, *113*, 11856−11865.
(55) Metz, S.; Kästner, J.; Sokol, A. A.; Keal, T. W.; Sherwood, P. ChemShell - a Modular Software Package for QM/MM Simulations. *WIREs Comput. Mol. Sci.* **2014**, *4*, 101−110.
(56) Cornell, W. D.; Cieplak, P.; Bayly, C. I.; Kollman, P. A. Application of RESP Charges To Calculate Conformational Energies, Hydrogen Bond Energies, and Free Energies of Solvation. *J. Am. Chem. Soc.* **1993**, *115*, 9620−9631.
(57) Bayly, C. C. I.; Cieplak, P.; Cornell, W. D.; Kollman, P. A. A Well-Behaved Electrostatic Potential Based Method Using Charge Restraints for Deriving Atomic Charges: The RESP Model. *J. Phys. Chem.* **1993**, *97*, 10269−10280.
(58) Stephens, P. J.; Devlin, F. J.; Chabalowski, C. F.; Frisch, M. J. Ab Initio Calculation of Vibrational Absorption and Circular Dichroism Spectra Using Density Functional Force Fields. *J. Phys. Chem.* **1994**, *98*, 11623−11627.
(59) Hehre, W. J.; Ditchfield, R.; Pople, J. A. Self-Consistent Molecular Orbital Methods. XII. Further Extensions of Gaussian-Type Basis Sets for Use in Molecular Orbital Studies of Organic Molecules. *J. Chem. Phys.* **1972**, *56*, 2257−2261.
(60) Hariharan, P. C.; Pople, J. A. The Influence of Polarization Functions on Molecular Orbital Hydrogenation Energies. *Theor. Chim. Acta* **1973**, *28*, 213−222.
(61) Retegan, M.; Neese, F.; Pantazis, D. A. Convergence of QM/MM and Cluster Models for the Spectroscopic Properties of the Oxygen-Evolving Complex in Photosystem II. *J. Chem. Theory Comput.* **2013**, *9*, 3832−3842.
(62) Weigend, F.; Ahlrichs, R. Balanced Basis Sets of Split Valence, Triple Zeta Valence and Quadruple Zeta Valence Quality for H to Rn: Design and Assessment of Accuracy. *Phys. Chem. Chem. Phys.* **2005**, *7*, 3297−3305.
(63) Grimme, S.; Antony, J.; Ehrlich, S.; Krieg, H. A Consistent and Accurate Ab Initio Parametrization of Density Functional Dispersion Correction (DFT-D) for the 94 Elements H-Pu. *J. Chem. Phys.* **2010**, *132*, 154104.
(64) Zhao, Y.; Truhlar, D. G. The M06 Suite of Density Functionals for Main Group Thermochemistry, Thermochemical Kinetics, Noncovalent Interactions, Excited States, and Transition Elements: Two New Functionals and Systematic Testing of Four M06-Class Functionals and 12 Other Functions. *Theor. Chem. Acc.* **2008**, *120*, 215−241.
(65) Tao, P.; Fisher, J. F.; Shi, Q.; Vreven, T.; Mobashery, S.; Schlegel, H. B. Matrix Metalloproteinase 2 Inhibition: Combined Quantum Mechanics and Molecular Mechanics Studies of the Inhibition Mechanism of (4-Phenoxyphenylsulfonyl)methylthiirane and Its Oxirane Analogue. *Biochemistry* **2009**, *48*, 9839−9847.

DOI: 10.1021/acs.jctc.6b00727
J. Chem. Theory Comput. 2017, 13, 1102−1107